0026-895X/06/7001-8–15$20.00
MOLECULAR PHARMACOLOGY
Copyright © 2006 The American Society for Pharmacology and Experimental Therapeutics
Mol Pharmacol 70:8–15, 2006

Vol. 70, No. 1
24380/3119670
Printed in U.S.A.

ACCELERATED COMMUNICATION

The Aryl Hydrocarbon Receptor Signaling Pathway Is Modified through Interactions with a Kelch Protein

Elizabeth E. Dunham, Emily A. Stevens, Edward Glover, and Christopher A. Bradfield

McArdle Laboratory for Cancer Research, University of Wisconsin Medical School, Madison, Wisconsin

Received March 16, 2006; accepted March 31, 2006

ABSTRACT

The aryl hydrocarbon receptor (AHR) is a ligand-activated transcription factor with important roles in metabolic adaptation, dioxin toxicology, and vascular development. To understand the details of this signal transduction pathway, we have used the yeast two-hybrid system to identify proteins that physically interact with the AHR in a ligand-dependent manner. Using this strategy, we identified a novel modifier of the AHR signaling pathway that we named Ah-receptor associated protein 3 (ARA3). Coexpression of ARA3 with an AHR chimera in yeast and mammalian cells enhances signaling in response to agonists. The human full-length cDNA previously was described as influenza virus nonstructural protein-1 binding protein (NS1BP). This protein contains four apparent domains—a "broad complex/tramtrack/bric-a-brac" (BTB) domain, a "kelch" domain, a "BTB and C-terminal kelch" (BACK) domain, and an intervening region (IVR). The carboxyl terminus of the AHR "Per-ARNT-Sim" (periodicity/AHR nuclear translocator/simple-minded) domain and the BACK/IVR domains of ARA3 mediate the AHR-ARA3 interaction. The BACK/IVR domains of ARA3 also are sufficient to modify AHR signaling in yeast and mammalian cells. In an effort to provide a preliminary model of NS1BP activity in AHR signaling, we demonstrate that NS1BP regulates the concentration of functional AHR in mammalian cells.

The aryl hydrocarbon receptor (AHR) is a member of the basic helix-loop-helix *Per-Arnt-Sim* (bHLH-PAS) superfamily. Upon binding ligands, the AHR mediates an adaptive metabolic response by up-regulating the transcription of a battery of xenobiotic metabolizing enzymes, including the cytochromes P450, CYP1A1, CYP1A2, and CYP1B1 (Schmidt and Bradfield, 1996). When stimulated by high-potency agonists, such as 2,3,7,8-tetrachlorodibenzo-*p*-dioxin (TCDD), the AHR mediates an additional toxic response that includes hepatocellular damage, thymic involution, teratogenesis, chloracne, and cancer (Pohjanvirta and Tuomisto, 1994; Fernandez-Salguero et al., 1996). It has been shown that the AHR also plays an important role in vascular development. In this regard, patent *ductus venosus* is observed in 100% of mice with a null allele at the *Ahr* locus (Lahvis et al., 2005). The presentation of vascular aberrations in AHR-mutant mice is consistent with the idea that the AHR is activated by an unknown endogenous ligand.

The AHR signaling pathway is understood at a basic level. In the absence of ligand, the AHR has a higher affinity for the cytosol, where it exists in a complex with the 90-kDa heat shock protein and the cochaperones ARA9 (also known as AIP1 or XAP2) and p23 (Wilhelmsson et al., 1990; Ma and Whitlock, 1997; Carver et al., 1998; Meyer et al., 1998; Kazlauskas et al., 1999). Upon ligand binding, the AHR attains a higher affinity for the nuclear compartment, where it dimerizes with another bHLH-PAS protein known as the AHR nuclear translocator (ARNT) (Reyes et al., 1992). The transcriptional activity of the AHR-ARNT heterodimer is modulated through interactions with cofactors such as SRC-1 and RIP140 (Kumar et al., 1999; Beischlag et al., 2002). The

This work was supported by National Institutes of Health grants R37-ES005703, T32-CA009135, and P30-CA014520.
Article, publication date, and citation information can be found at http://molpharm.aspetjournals.org.
doi:10.1124/mol.106.024380.

ABBREVIATIONS: AHR, aryl hydrocarbon receptor; bHLH, basic helix-loop-helix; PAS, Per-Arnt-Sim (periodicity/Arnt/simple-minded); Arnt, aryl hydrocarbon receptor nuclear; translocator; ARA3, aryl hydrocarbon receptor associated 3; ARA9, aryl hydrocarbon receptor associated 9; NS1BP, influenza virus nonstructural protein 1 binding protein; TAD, transcription activation domain; PCR, polymerase chain reaction; βNF, β-naphthoflavone; DOC, deoxycorticosterone; ANOVA, analysis of variance; TCDD, 2,3,7,8-tetrachlorodibenzo-*p*-dioxin; MOPS, 3-(*N*-morpholino)propanesulfonic acid; BTB, broad complex/tramtrack/bric-a-brac; IVR, intervening region; AA, amino acid(s).

AHR pathway can be attenuated by two mechanisms, proteasome-dependent degradation of the AHR and the AHR-mediated transcription of a dominant-negative bHLH-PAS protein known as the *Ah* receptor repressor (Davarinos and Pollenz, 1999; Mimura et al., 1999).

In previous studies, we have demonstrated that the yeast *Saccharomyces cerevisiae* is an excellent model of AHR signal transduction (Carver et al., 1994; Yao et al., 2004). In an effort to identify unknown components of the AHR signaling pathway, we have been employing a yeast-two-hybrid strategy to screen for proteins that interact with the AHR in a ligand-dependent manner. This approach has led to the identification of ARA9, now a proven AHR cochaperone (Ma and Whitlock, 1997; Bell and Poland, 2000; LaPres et al., 2000; Petrulis et al., 2000). As a result of this earlier success, we began characterizing the second clone identified in our yeast-two-hybrid assay [i.e., *Ah receptor associated 3* (*ARA3*)] (Carver and Bradfield, 1997). Herein, we characterize the AHR-ARA3 interaction and its effect on AHR signaling in yeast and mammalian cells.

Materials and Methods

Oligonucleotide sequences are shown in Table 1.

Strains and Plasmids. *Saccharomyces cerevisiae* strain L40 (*Mat* a, *his3Δ200*, *trp1–901*, *leu2–3*, *112*, *ade2*, *LYS2*::*(lexAop)$_4$-HIS3*, *URA3*::*(lexAop)$_8$-lacZ*, *gal80*) was used in both the yeast two-hybrid assays and the pharmacology experiments (Vojtek et al., 1993). The plasmid *pBTM116* is a 2-μm TRP-marked yeast expression vector for making LexA DNA binding domain (LexA) fusion proteins under regulation of the *ADH1* promoter (Bartel et al., 1993). The plasmid *pYX242* (Novagen, Madison, WI) is a 2-μm LEU-marked yeast expression vector under the regulation of the *TP1* promoter. The plasmid *pACT* (Clontech, Mountain View, CA) is a 2-μm LEU-marked vector used to make GAL4 transcription activation domain (TAD) fusion proteins. The plasmid *pSPORT* AHR (PL65) was used as a template for any AHR PCR amplifications and has been described previously (Dolwick et al., 1993). The plasmid *pYX* AHR (PL1033) was constructed by PCR using OL1378 and OL1379 using PL65 as the template and was subcloned from *pGEMT* (Promega, Madison, WI) using XhoI and SalI into the SalI site of *pYX242*. The plasmid *pACT* ARA3 (PL792) was isolated as described previously from a two-hybrid screen with a human B-cell library using *pBTM* LexA-AHRΔTAD (PL739) as the bait construct (Carver and Bradfield, 1997). The plasmids *pBTM* LexA-ARA3 (PL1416) and *pYX* ARA3 (PL1468) were constructed by PCR amplification of PL792 using OL1469 and OL926, ligated into *pGEMT*, then subcloned into EcoRI and SalI of *pBTM116* or *pYX242*. The plasmids *pSGBCU* ARNT (PL574), *pBTM* LexA-ΔbHLHAHR (PL703) and *pY2* N-LexA-C (PL740) have been described previously (Carver et al., 1994; Hogenesch et al., 1997; LaPres et al., 2000).

Transformations and Library Screening. Transformations into *S. cerevisiae* strain L40 were performed by a modified lithium acetate method as described previously (Carver et al., 1994). The plates were incubated for 2 days at 30°C and then replica-plated onto media containing 100 μl of the vehicle dimethyl sulfoxide or 100 μl of various concentrations of the ligand β-naphthoflavone (βNF) or deoxycorticosterone (DOC). After 2 days of growth, triplicate groups of 6 to 10 colonies for each condition were resuspended in 500 μl of buffer Z (60 mM Na_2HPO_4, 40 mM NaH_2 PO_4, 10 mM KCl, 1 mM $MgSO_4$, and 35 mM β-2-mercaptoethanol). The A_{600} was measured on a 1:10 dilution of this cell suspension to determine cell density, and β-*galactosidase* (*lacZ*) expression was determined on 150 μl of this cell suspension as described previously (Carver et al., 1998). Percentage of maximal response was plotted using the program Prism (GraphPad Software, San Diego, CA). Statistical significance also was determined with ANOVA followed by Tukey's multiple comparison test in Prism.

Cloning 5′-End of Human ARA3. The 5′-end of human ARA3 cDNA was obtained by a 5′-rapid amplification of cDNA ends procedure using Marathon-Ready human heart cDNA library kit per the manufacturer's protocol (Clontech). The OL1191 was used as the gene-specific primer along with the vector-specific primer AP1 to generate a 5′-end cDNA product. The resulting product was cloned into *pGEMT* and sequenced. To generate the full-length human ARA3 cDNA (FLARA3), the 5′-rapid amplification of cDNA ends EcoRI/XbaI fragment was cloned into PL1425 to generate *pGEMT*-FL ARA3 (PL1424).

ARA3 Deletions. The T7-tagged ARA3 constructs were created by including the T7 epitope (MASMTGGQQMG) on the 5′ end of the sense oligonucleotide 2006 used to PCR-amplify these constructs. The sense oligonucleotide 1469 was used to amplify products without a T7 tag to generate LexA fusions. All ARA3 deletions were created by PCR amplification of PL792 and subcloned from *pGEMT* into *pYX242* and *pBTM116* using the restriction enzymes EcoRI and SalI. The following antisense oligonucleotides were used to delete the ARA3 kelch repeats are as follows: OL1886 to delete the last two kelch repeats, OL1887 to delete last four kelch repeats, and OL1888 to delete all six kelch repeats. The deleted kelch repeat constructs are as follows: *pYX*, T7ARA3ΔKR5–6 (PL1443), *pBTM*, LexA-ARA3ΔKR5–6 (PL1451); *pYX*, T7ARA3ΔKR3–6 (PL1444); *pBTM*, LexA-ARA3ΔKR3–6 (PL1452); *pYX*, T7ARA3ΔKR1–6 (PL1445); and *pBTM*, LexA-ARA3ΔKR1–6 (PL1453). The plasmid *pYX* T7ARA3 (PL1417) was created by PCR amplification of the template PL792 with OL2006 and OL926. The T7FLARA3 construct was created by PCR amplification using OL1490 and OL926 of the template PL1424 and ligated into *pTarget* (Promega). The FLARA3 insert was first subcloned into *pET17B* (Novagen) using EcoRI and SalI to create the

TABLE 1
Oligonucleotide sequences

OL163	CCCAAGCTTACGCGTGCAGTGGTCTCTGAGTGGCGATGATGTAATCTGG
OL180	GCGTCGACTGATGAGCAGCGGCGCCAACATCACC
OL258	GCCGTCGACGCGGCCGCGAAGTCTAGCTTGTGTTTGG
OL392	CCGCTCGAGTGATGAGCAGCGGCGCCAACATCACC
OL822	TAATACGACTCACTATAGGG
OL926	GCTTGTGTTGCTGTTAG
OL1191	CCTCAGCCTGTCCACGAACTACCCTTGGATGATC
OL1378	GATCCCTCGAGCCACCATGAGCAGCGGCGC
OL1379	GATGCTCGAGGTGGCCAATGCTGCTC
OL1469	GGCGAATTCACCATGGATCGAGTAAAGC
OL1490	GGCCAATTCACCATGATTCCCAATGG
OL1886	CCTTATCCTCGCCTAGCCACATTC
OL1887	CCTTAACAACGGTTAGTTCTCAAC
OL1888	CCTTATCGTGCGTACTGCATAGGAG
OL2006	GGGAATTCATTATGGCTAGCATGACTGGTGGACAGCAAATGGGTATGGATGGAGTAAAGCAGGTTTGTGG
OL2372	GCTCGAGTTATCCGGTAGCAAACATGAAGGGCAG

in-frame fusion with the amino terminus T7 tag. This T7FLARA3 construct was then PCR-amplified with OL822 and OL926 and cloned into *pTarget* (PL1430). The PL1430 was first digested with XhoI, and then the XhoI overhangs were filled in with the Klenow fragment. This T7FLARA3 insert was then subcloned into the EcoRV and SmaI sites of *pYX242* to create *pYX* T7FLARA3 (PL1442). The LexA fusion of FLARA3 was constructed by subcloning the insert from *pTarget* FLARA3 (PL1430) using EcoR I and SalI into the EcoRI/SalI sites of *pBTM116* to create *pBTM* LexA-FLARA3 (PL1456). Expression of ARA3 and the amino and carboxyl-terminal deletions of ARA3 were confirmed by Western blot analysis on yeast cell extracts as described previously (Hogenesch et al., 1997).

Hydroxylamine Mutagenesis. Hydroxylamine mutagenesis was performed as described previously (Garabedian, 1993). A 1 M solution of hydroxylamine was prepared immediately before use in 50 mM EDTA. Equal volumes of 1 M hydroxylamine solution and 1 M potassium phosphate buffer were mixed together with 2 μg of purified plasmid DNA *pYX* T7ARA3 (PL1417) or the control plasmid *pBluescript* II ± (Invitrogen). The hydroxylamine/DNA mixture was incubated at 25°C for 48 h. The DNA was purified over a G50 column (Roche, Basel, Switzerland) and transformed into JM109 bacteria. Plasmid DNA from the bacteria was purified on a maxiprep column (QIAGEN, Valencia, CA). The mutagenized PL1417 was then transformed with PL703 into the L40 strain of *S. cerevisiae* by modified lithium acetate method as described above. The wild-type PL1417 and the empty vector *pYX242* were also transformed with PL703 to serve as controls for the experiment. All of the yeast transformations were replica-plated onto media containing 10 μM βNF. Activation of the *lacZ* reporter was determined. Any mutant white colonies after 1 h were picked and rescued into HB101 bacteria. All rescued plasmids were retransformed into L40 yeast along with PL703 to confirm the loss of function and a Western analysis was performed on yeast extracts to confirm the expression. Any mutants expressed at wild-type levels were then sequenced to identify the mutation. The mutants, *pYX* T7ARA3V198M (PL1448) and *pYX* T7ARA3E288K (PL1449) were PCR-amplified using OL1469 and OL926, TA-cloned into pGEMT, and subcloned into pBTM116 to create *pBTM* ARA3 V198M (PL1457) and *pBTM* ARA3 E288K (PL1458).

AHR Deletions. The plasmid *pSPORT* AHRΔ313 (PL145) has been described previously (Dolwick et al., 1993). The plasmid *pBTM* LexA-ΔbHLHAHRΔTAD (PL1297) was created by deleting the EcoRI fragment from *pBTM* LexA-AHRΔTAD (PL739). The AHR deletions *pBTM* LexA-AHRΔ425 (PL1301) and *pBTM* LexA-AHRΔ402 (PL1377) were constructed by PCR amplification of the template PL65 using OL392 as the sense primer and OL163 and OL2372, respectively. All were cloned into pGEMT and subcloned into the SalI site of pBTM116 using XhoI and SalI. The plasmid *pBTM* LexA-ΔbHLHAHRΔ402 (PL1324) was created by deleting the EcoRI fragment from *pBTM* LexA-AHRΔ402. The plasmid *pBTM* LexA-AHRΔ313 (PL1300) was constructed by PCR amplification using OL1378 and OL822 of the template PL145, and the insert was subcloned from pGEMT into the SalI site of pBTM116 using XhoI and SalI. The plasmid *pBTM* LexA-AHRΔ516 (PL1322) was generated by PCR amplification using OL180 and OL258 of the template PL65 and the insert was subcloned from pGEMT using SalI into the SalI site of *pGAD424* (Clontech, Palo Alto, CA). The pGAD AHRΔ516 (PL718) construct was digested with XmaI, and the PstI and the AHR insert was subcloned into the SmaI and PstI sites of pBTM116.

Mammalian Cell-Culture Assays. The plasmid *pSG* Gal4-ΔbHLHAHR (PL118) has been described previously (Jain et al., 1994). The *pTarget* T7ARA3 (PL1797) and *pTarget* T7ARA3Δkelch (PL1429) constructs were generated by PCR amplification of PL792 using OL2006/OL926 and OL2006/OL1888. PL1430 is described above. The plasmid *pG5* Luciferase (Promega) is a luciferase reporter construct containing five upstream GAL4 DNA response elements. The PL186 is a *β-galactosidase* expression vector driven by a Simian virus-40 promoter. Mammalian cell culture experiments were performed in Cos-1 cells maintained at 37°C and 5% CO_2 in Dulbecco's modified Eagle's medium supplemented with 10% fetal bovine serum, penicillin (0.1 unit/ml), and streptomycin (0.1 μg/ml), HEPES buffer (10 mM), minimal essential amino acids (0.1 mM), and sodium pyruvate (1 mM) (Invitrogen). Transient transfections were carried out in six-well plates with Effectene (QIAGEN) per manufacturer's instructions. DNA used in transfections consisted of 800 ng of PL118, 800 ng of PL1797, PL1429, PL1430, or an empty vector. In addition, 800 ng of *pG5* Luciferase was used as a reporter and 600 ng of PL186 to control for transfection efficiency. Media were changed at 4 h after transfection, and at 24 h after transfection 10 nM TCDD or dimethyl sulfoxide (vehicle control) was added. Cells were incubated for another 24 h and harvested using Reporter Lysis Buffer (Promega). Luciferase and β-galactosidase activity were measured with the appropriate assay system per manufacturer's instructions (Promega).

Transient Transfection for Receptor Binding. Cos-1 cells were maintained and transfected as described above with the following modifications. Cells were maintained in 10-cm^2 dishes and transfected with 300 ng of PL118 and 300 ng of PL1429 or an empty vector. Forty hours after transfection, the cells were harvested with trypsin and washed twice with PBS. Cell pellets were resuspended in buffer consisting of 25 mM MOPS, pH7.4, 1 mM dithiothreitol, 1 mM EDTA, 5 mM EGTA, 0.02% NaN_3, and 10% glycerol) supplemented with 10 mM Na_2MoO_4. Samples were disrupted using a Dounce homogenizer in the presence of a protease inhibitor cocktail (Roche). The samples were subjected to centrifugation at 14,000*g* (10 min, 4°C). An additional centrifugation (100,000*g*, 60 min, 4°C) was performed on the supernatants to obtain the soluble or "cytosolic" fraction. Protein concentrations of the cytosols were determined by Coomassie Reagent assay (Pierce, Rockford, IL), and samples were diluted to a final protein concentration of 1 mg/ml.

Photoaffinity Labeling. The photoaffinity labeling of the AHR was carried out as described previously (Bradfield et al., 1988). In brief, 1 nM 2-azido-3-[^{125}I]iodo-7,8-dibromodibenzo-*p*-dioxin, the photoaffinity ligand, was added to 150 μg/ml cytosolic protein and incubated for 30 min at 20°C, then 5 min on ice. Unbound ligand was removed with charcoal/dextran (10%/1%, w/v). The receptor/ligand complex was cross-linked by exposure to ultraviolet light (310 nm, 80 W, 4 cm) for 30 s. Four milliliters of acetone was added and the mixture was incubated for 16 h at −20°C. The acetone precipitate was removed by centrifugation (2000*g*, 10 min, 4°C), and the pellet was washed with 90% acetone/water. The samples were resuspended in electrophoresis sample buffer and run on a 7.5% SDS-polyacrylamide gel electrophoresis gel. Gels were analyzed by autoradiography, and appropriate bands were cut out and counted on a Minaxi gamma counter (PerkinElmer Life and Analytical Sciences, Boston, MA). Statistical Significance was determined with a Student's *t* test.

Results and Discussion

We previously reported a modified yeast two-hybrid assay to screen for proteins that interact with the AHR in a ligand-

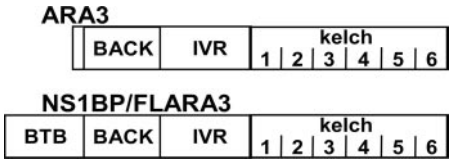

Fig. 1. Analysis of the ARA3 cDNA revealed three characterized protein domains. The ARA3 yeast two hybrid clones originally identified in our screen encoded a 531-AA protein. There was no Kozak consensus initiation ATG present. Therefore, the human full-length ARA3 (FLARA3) was cloned from a human heart cDNA library and sequenced. FLARA3 is 642 AA long, whereas the original ARA3 clone was missing the first 111 AA. Similarity searches identified FLARA3 as a protein originally called NS1BP. The NS1BP/FLARA3 protein contains a BTB domain from AA 22 to 129, a BACK domain from AA 134 to 233, and a kelch domain consisting of six imperfect 50-AA kelch repeats from AA 357 to 635 (http://www.sanger.ac.uk). A low homology region exists between the BACK and kelch domains that we refer to as the IVR.

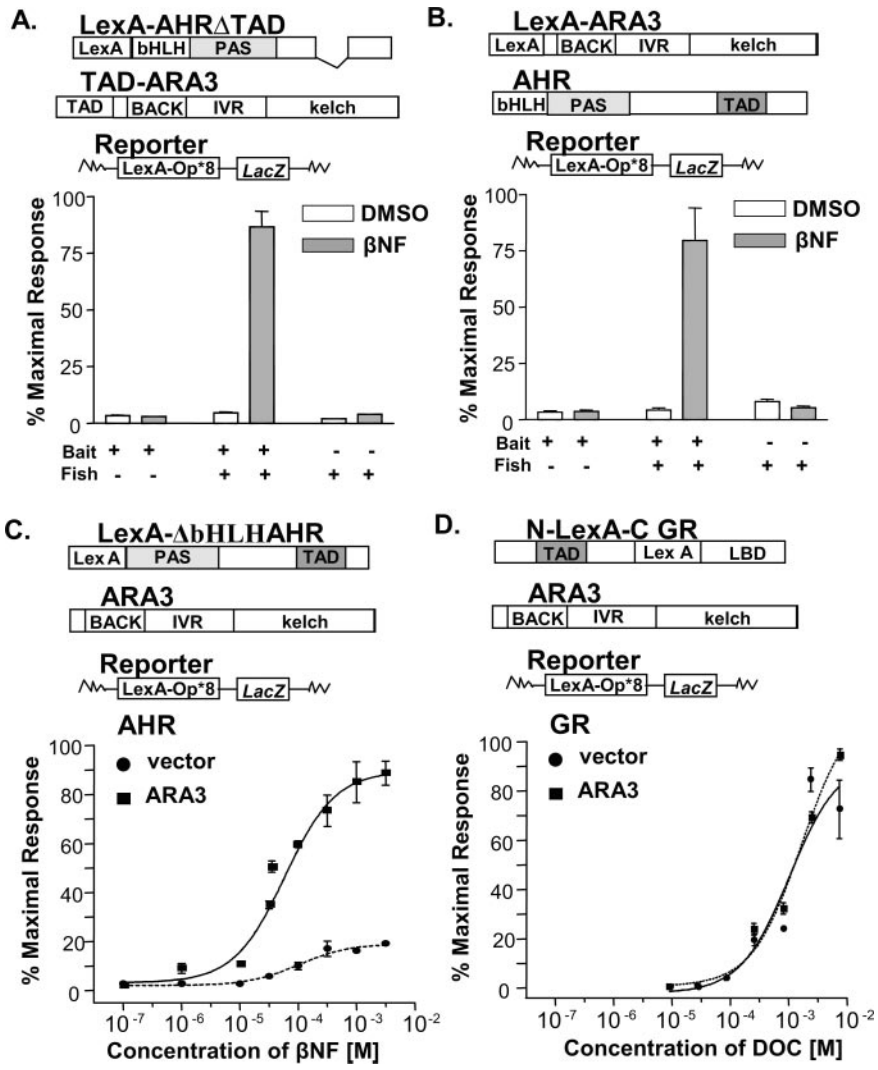

Fig. 2. ARA3 interacts with AHR ligand-dependently and modifies the AHR signaling pathway. The L40 yeast, expressing an integrated β-galactosidase (*lacZ*) reporter, were transformed with constructs depicted above each graph and treated with the appropriate ligand or vehicle. LacZ activity was determined and normalized to the number of cells. Values are the average of three replicates and represent at least two independent experiments. A, yeast-two-hybrid assay. LexA-AHRΔTAD, TAD-ARA3, or control vectors were transformed in yeast and treated with either 1 mM βNF or vehicle. B, a reverse-two-hybrid assay was performed as in A. C, aryl hydrocarbon receptor pharmacology. Yeast were transformed with the LexA-AHR chimera and ARA3 or control vector and treated with increasing concentrations of βNF. D, glucocorticoid receptor pharmacology. Yeast were transformed with the LexA-GR chimera and ARA3 or control vector and treated with increasing concentrations of DOC.

dependent manner. This screen of more than 700,000 human cDNAs yielded 10 positive clones (Carver and Bradfield, 1997). Sequence analysis revealed that five of these clones represented a unique cDNA that was designated *ARA9*. The other five clones represented a second distinct cDNA that we designated *ARA3*. Given that the importance of ARA9 in AHR signaling has been demonstrated repeatedly since this initial report, we returned to characterize the function of ARA3 (Ma and Whitlock, 1997; Bell and Poland, 2000; La-Pres et al., 2000; Petrulis et al., 2000).

Analysis of the ARA3 cDNA. Sequence analysis of the five ARA3 cDNAs indicated that they were identical and encoded a large open reading frame of 531 amino acids. Given that a consensus initiation ATG codon was not identified in the original cDNA, the 5′ end was amplified by PCR of a human heart library (Clontech). As the result of this experiment, the full-length open reading frame of ARA3 (FLARA3) was found to be 642 amino acids in length and contained a consensus initiation ATG codon with an upstream, in-frame stop codon (Kozak, 1987) (Fig. 1).[1] Comparison of FLARA3 with other proteins in the GenBank database revealed a preliminary domain map. At the N terminus of FLARA3 is a broad complex/tramtrack/bric-a-brac (BTB) domain found in several transcriptional regulators and non–DNA-binding proteins (Zollman et al., 1994; Collins et al., 2001). In addition to mediating hetero-/homodimerization, the BTB domain has been shown to recruit corepressors and histone deacetylases (Melnick et al., 2002). At its C terminus, ARA3 harbors a "kelch" domain, consisting of six imperfect repeats of approximately 50 amino acids. This domain has been shown to have the potential to form a β-propeller structure (Adams et al., 2000). Like many other BTB-kelch proteins, FLARA3 also harbors a motif referred to as a "BTB and C-terminal kelch" homology domain (BACK) (Stogios and Prive, 2004). In some BTB-kelch proteins, the BACK domain aids in the interaction of the BTB domain with ubiquitin-ligase complexes (Stogios and Prive, 2004; Furukawa and Xiong, 2005). A fourth region with no significant amino acid sequence homology exists between the BACK and kelch domains. We designate this domain as the "intervening region" (IVR).

Since the time of our initial report of ARA3, the human and mouse cDNAs have been reported by other laboratories. The human cDNA was first reported as an influenza virus NS1 binding protein (NS1BP) (Wolff et al., 1998). The murine NS1BP ortholog, designated Nd1, and a splice variant also were cloned in a screen for cDNAs differentially expressed in

[1] The sequences of ARA3 and NS1BP/FLARA3 have been submitted to GenBank under accession numbers DQ443529 and DQ443528, respectively.

neurons of *Ncx*-deficient mice that stabilize actin filaments (Sasagawa et al., 2002). Given this provenance, we now refer to FLARA3 as NS1BP and use the ARA3 designation to refer to the clone obtained from the original two-hybrid screen (Fig. 1). Murine NS1BP transcripts were previously found in all tissues examined with the highest expression in the heart, kidney, and intestines (Sasagawa et al., 2002). By Northern blot analysis on murine tissue, we also detected NS1BP mRNA in the heart and kidney, as well as muscle, lung, testis, and brain (data not shown).

AHR and ARA3 Proteins Interact. To confirm the ligand-dependent nature of the AHR-ARA3 interaction, plasmids harboring a LexA-AHR fusion (LexA-AHRΔTAD) and a TAD ARA3 fusion (TAD-ARA3) were transformed into the L40 reporter strain. The separation of the LexA DNA-binding domain and the TAD on two proteins requires that the two proteins interact for reporter activation. A 21-fold increase in β-galactosidase (LacZ) reporter activity was observed when the cotransformed yeast were exposed to the AHR agonist βNF (Fig. 2A). To determine whether this interaction was context-dependent, the reverse-two hybrid experiment was performed. To this end, a LexA-ARA3 fusion (LexA-ARA3) was screened against the full-length AHR containing its cognate TAD (AHR). Again, an 18.5-fold increase in LacZ reporter activity was seen when these constructs were coexpressed in the presence of βNF (Fig. 2B).

Ahr Signaling Is Enhanced in the Presence of ARA3. We have previously shown that an AHR chimera harboring its cognate TAD, LexA-ΔbHLHAHR, displays a pharmacological response to βNF in yeast similar to that of the AHR/ARNT heterodimer in mammalian cells (Carver et al., 1994). By removing the bHLH domain of AHR, the dependence of AHR on ARNT is removed. To determine the effect of ARA3 on AHR signaling, L40 yeast were transformed with LexA-ΔbHLHAHR along with ARA3 cDNA or control vector. When grown in the presence of increasing concentrations of βNF, we observed that coexpression of ARA3 influenced the shape of the dose-response curve significantly. In the presence of ARA3, the EC_{50} decreased from 1×10^{-4} to 6×10^{-5} and the maximal response increased approximately 5-fold. This change in dose-response is consistent with the idea that ARA3 increases the concentration of AHR available to bind ligand and activate transcription (Fig. 2C) (Bourne and von Zastrow, 2001). To determine whether the effect of ARA3 was specific to AHR signaling, a similar pharmacology experiment was performed with a LexA fusion of the glucocorticoid receptor ((GR)N-LexA-CGR) with its ligand DOC. Coexpression of ARA3 did not influence GR signaling in this assay (Fig. 2D).

The BACK/IVR Domains of NS1BP/FLARA3 Modify AHR Signaling. We first mapped the functional domains of NS1BP/FLARA3 by examining specific deletions for their effect on AHR signaling in yeast. The deletions were constructed with a T7-epitope tag to monitor protein expression levels. In this system, LexA-ΔbHLHAHR was cotransformed with each NS1BP/FLARA3 deletion. We observed that NS1BP/FLARA3 increased the signaling of the AHR chimera by 2-fold ($P < 0.01$), whereas the original ARA3 cDNA, with the BTB domain deleted, increased AHR signaling by approximately 10-fold ($P < 0.001$). This suggests that the BTB

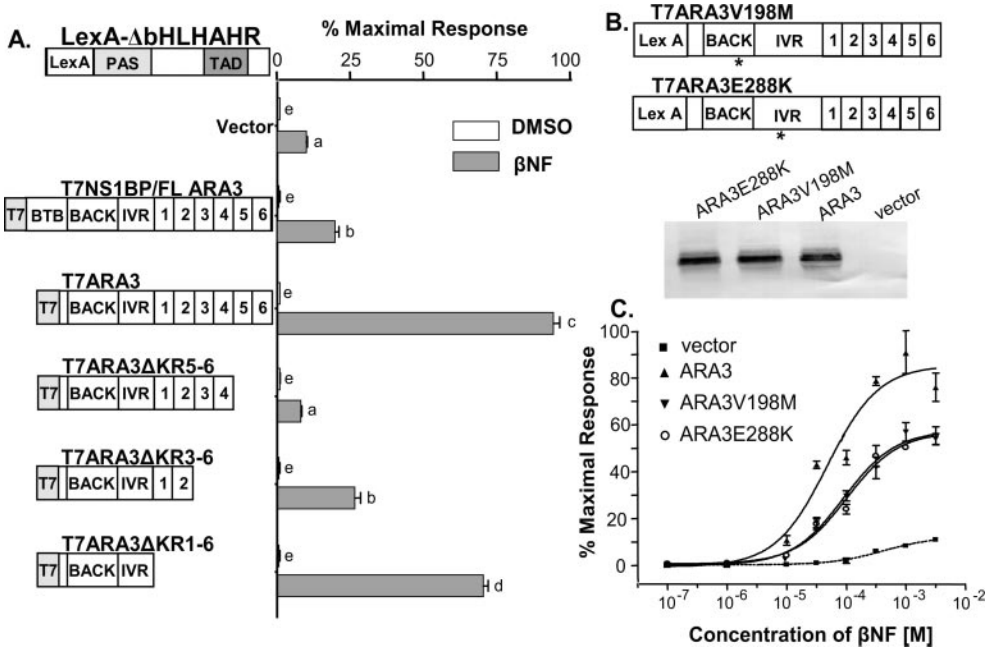

Fig. 3. The BACK/IVR domains of NS1BP/FLARA3 modify AHR signaling. The L40 yeast, expressing an integrated β-galactosidase (*lacZ*) reporter, were transformed with the AHR chimera LexA-ΔbHLHAHR and T7-tagged ARA3 constructs or a vector control. LacZ activity was determined and normalized to the number of cells. Values are the average of three replicates and represent at least two independent experiments. A, AHR pharmacology. Yeast were transformed with the LexA-AHR chimera and ARA3 constructs or vector control and grown in the presence of 1 mM βNF or vehicle. Statistical significance was determined with ANOVA followed by Tukey's multiple comparison test in PRISM. The same subscript depicts values that are statistically the same ($P > 0.05$). Different subscripts designate a statistical difference in the values ($P < 0.01$). B, expression of ARA3 mutants. ARA3 point mutations were generated with hydroxylamine and screened as described under *Materials and Methods*. A schematic of the mutants is shown. To confirm protein expression levels of the mutant ARA3, a Western blot was performed on L40 yeast extracts. C, aryl hydrocarbon receptor pharmacology. The two ARA3 point mutants, an empty vector or ARA3 were transformed with LexA-ΔbHLHAHR exposed to increasing amounts of βNF.

domain inhibits the effect of ARA3 on AHR signaling. Deletion of the entire kelch domain resulted in only a modest (25%) reduction in signaling. An "all-or-nothing" effect was observed, with deletions of individual kelch repeats disrupting ARA3 function. This observation suggests that the kelch domain must be expressed in its entirety for normal folding and stability and that the kelch domain of ARA3 does not play an essential role in modifying AHR signaling (Fig. 3A).

To address potential effects on protein stability and folding caused by large deletions, we next used hydroxylamine to induce random mutations in ARA3 (Garabedian, 1993). To this end, a library of point mutants was cotransformed with LexA-ΔbHLHAHR in L40 yeast and plated onto media containing 10 μM βNF. Expression levels and size of the mutants were confirmed by Western blot analysis using a T7 antibody. All full-length mutants were sequenced, and two single point mutations were identified. One mutation resulted in a valine-to-methionine substitution at amino acid 198 (V198M) within the BACK domain, and the second resulted in a glutamate-to-lysine substitution at amino acid 288 (E288K) within in the IVR (Fig. 3B). A dose-response analysis revealed that both mutations yielded partial loss-of-function phenotypes, decreasing the maximal response by 35% and decreasing the effect on the EC_{50} by 50% (Fig. 3C). The point mutants further confirmed that the BACK/IVR domains of ARA3 represent the minimal effector domain.

The BACK/IVR Domains of NS1BP/FLARA3 Also Mediate the Interaction with AHR. We also mapped the NS1BP/FLARA3 domains that interact with AHR. In this series of experiments, we cloned the ARA3 deletions described above into the vector *pBTM116* to generate LexA fusions. These deletion constructs were then cotransformed with the AHR in yeast. In this assay, reporter induction occurs when the LexA ARA3 fusions physically interact with the AHR. As in Fig. 2B, LexA-ARA3 interacts with AHR in a ligand-dependent manner. In a manner similar to the pharmacology experiments in Fig. 3C, subdeletions of the kelch domain significantly disrupt the AHR-ARA3 interaction, whereas complete removal of the kelch domain reveals a mutant with near wild-type interaction activity (comparing LexA-ARA3ΔKR5–6 and 3–6 with LexA-ARA3ΔKR1–6). In addition, as in the pharmacology experiments in Fig. 3C, the two point mutations significantly inhibited the AHR-ARA3 interaction by 70% (Fig. 4A). We were unable to determine the role of the BTB domain of NS1BP on the interaction with AHR or whether NS1BP interacted with AHR at all, because LexA-NS1BP/FLARA3 activated the reporter independent of its interaction with AHR or the presence of ligand (Fig. 4B). The fact that expression of LexA-NS1BP led to reporter induction in the absence of ligand- or TAD-containing construct suggests that the BTB domain might allow NS1BP to heterodimerize with other transcription factors containing TADs. In summary, Figs. 3 and 4 demonstrate that the BACK/IVR domains of NS1BP/ARA3 are sufficient for the AHR-ARA3 interaction, as well as the ability of ARA3 to modify AHR signaling.

The C Terminus of the AHR PAS Domain Interacts with ARA3. We used a series of AHR deletions to determine those regions important for its interaction with ARA3. We compared the AHR-ARA3 interaction to the interaction of AHR with its known dimerization partner ARNT. We observed that the C terminus of the AHR PAS domain, specifically AA 289 to 403, is essential for the AHR-ARA3 interaction. In contrast, a distinct region, AA 380 to 492, is required for the AHR-ARNT interaction in this system. The bHLH of AHR also is necessary for the AHR-ARNT interaction, but its role in the AHR-ARA3 interaction is less clear. The bHLH inhibits the interaction of ARA3 with LexA-AHRΔTAD but is necessary for ARA3 to interact with LexA-AHRΔ402 (Fig. 5). We have demonstrated previously that AA 130 to 491 of AHR mediate the AHR-ARA9 interaction (Carver et al., 1998). Taken in sum, these data suggest that the AHR uses overlapping but distinct domains for interactions with ARA3, ARA9, and ARNT.

ARA3 Increases Signaling of an Ahr Chimera in Mammalian Cells. The influence of NS1BP/FLARA3 on signaling by a Gal4-AHR fusion first was investigated in Cos-1 cells by transfections of a *luciferase* reporter gene driven by the Gal4 promoter. In these experiments, the

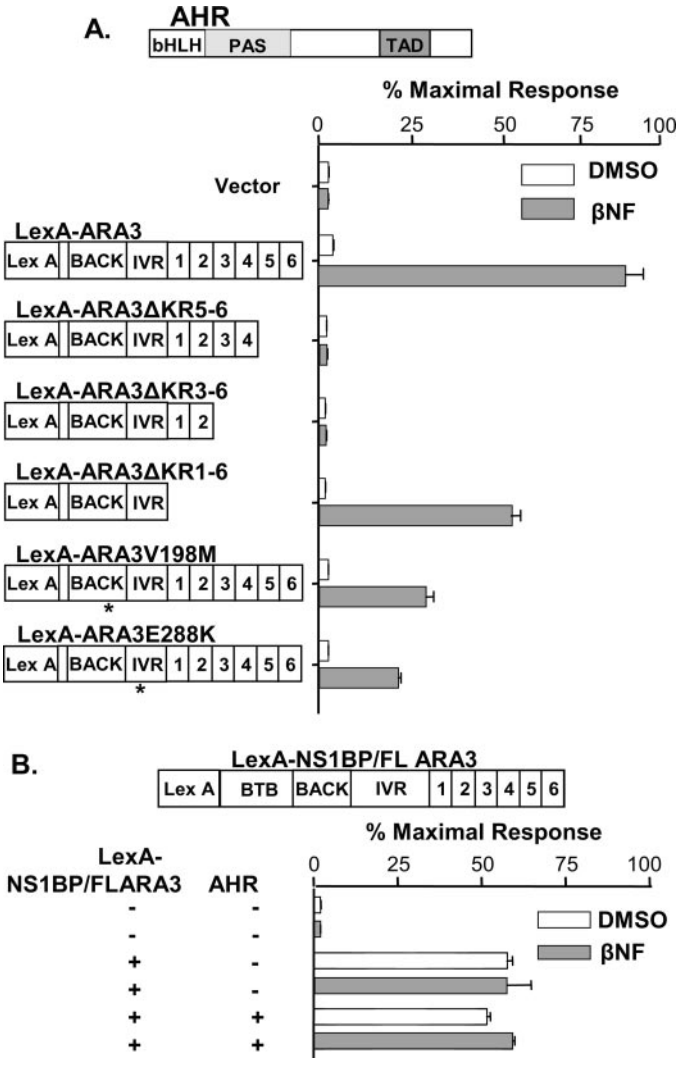

Fig. 4. The BACK/IVR domains of NS1BP/FLARA3 also mediate the interaction with AHR. The L40 yeast, expressing an integrated β-galactosidase (*lacZ*) reporter, were transformed with full-length AHR and LexA fusions of the ARA3 constructs or a vector control. The yeast were exposed to 1 mM βNF or vehicle. LacZ activity was determined and normalized to the number of cells. Values are the average of three replicates and represent at least two independent experiments. A, yeast-two-hybrid assay. An asterisk indicates the location of point mutations. B, control yeast-two-hybrid assay.

ΔbHLHAHR was fused to the DNA binding domain of Gal4 (Gal4-ΔbHLHAHR) and cotransfected with T7ARA3, T7NS1BP/FLARA3, T7ARA3ΔKR1–6, or vector control. The addition of NS1BP/FLARA3 increased signaling of the AHR chimera in response to TCDD by more than 2-fold ($P < 0.001$). In agreement with the results of the LexA-AHR chimera in yeast, removal of the BTB domain increased the modifier activity of ARA3 even further. That is, addition of the original ARA3 cDNA increased signaling of the AHR chimera in mammalian cells by almost 5-fold ($P < 0.001$) (Fig. 6A). The fact that NS1BP was significantly less effective on AHR chimera signaling than ARA3 provides further evidence that the BTB domain of ARA3 plays a negative role in AHR signaling.

The yeast pharmacology experiments depicted in Fig. 2C are consistent with the idea that ARA3 increases the concentration functional AHR in cells. An increase in AHR could account for the modifier activity of ARA3. Given that the BACK/IVR domains of NS1BP are sufficient to mediate the AHR-ARA3 interaction and represent the minimal effector domain of NS1BP, we tested the hypothesis that this region increases the concentration of functional AHR in mammalian cells. To this end, we transfected Cos-1 cells with the Gal4-AHR chimera in the presence of the NS1BP BACK/IVR domains or an empty vector and measured the amount of AHR with a radioactive ligand. That is, with a saturating concentration of ligand, we observed a 2.5-fold increase in the concentration of the AHR chimera in the presence of the NS1BP BACK/IVR ($P < 0.05$; Fig. 6B). These results demonstrate that the BACK/IVR domains of NS1BP do increase the functional concentration of AHR in the cytosol.

We have demonstrated that ARA3 binds AHR in a highly specific yeast-two-hybrid assay and enhances AHR signaling in yeast as well as mammalian cells. The dose-response analysis suggested that ARA3 increases the concentration of functional AHR. We have cloned full-length ARA3 and determined that it is the previously identified NS1BP without the BTB domain. Through a series of deletions and mutants, we have shown that the BACK/IVR of NS1BP is sufficient for its interaction with AHR and its effect on AHR signaling. In addition, we determined that the BACK/IVR domains in isolation increase the concentration of functional AHR in cells. It is noteworthy that deletion of the BTB domain significantly enhances the modifier activity of NS1BP.

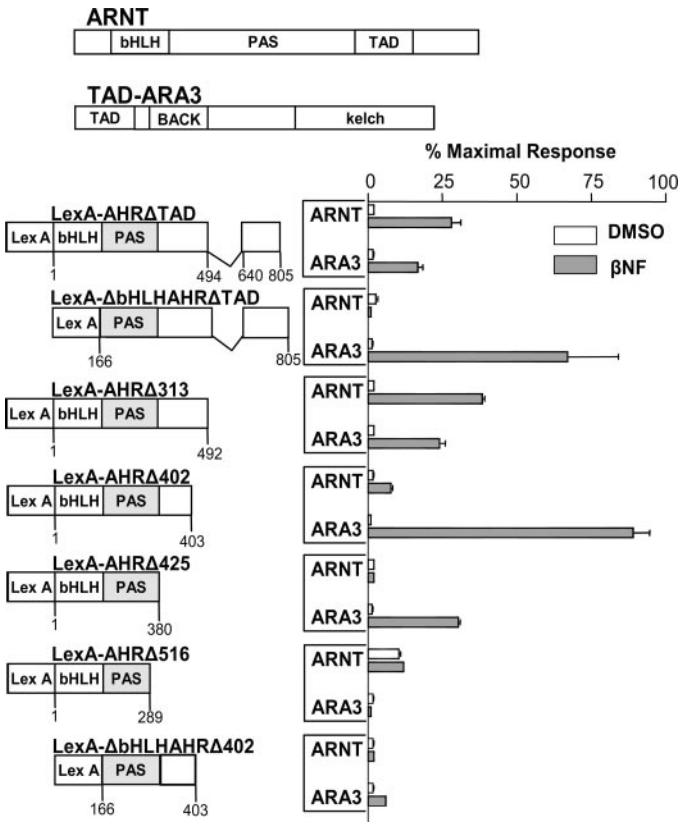

Fig. 5. The C terminus of AHR's PAS domain is necessary for the interaction with ARA3. The L40 yeast, expressing an integrated β-galactosidase (*lacZ*) reporter, were transformed with full-length ARNT or TAD-ARA3 and LexA fusions of a AHR deletion series. The yeast were exposed to 1 mM βNF or vehicle. LacZ activity was determined and normalized to the number of cells. Values are the average of three replicates and represent at least two independent experiments. The regions of AHR important for its interaction with ARA3 and ARNT were compared.

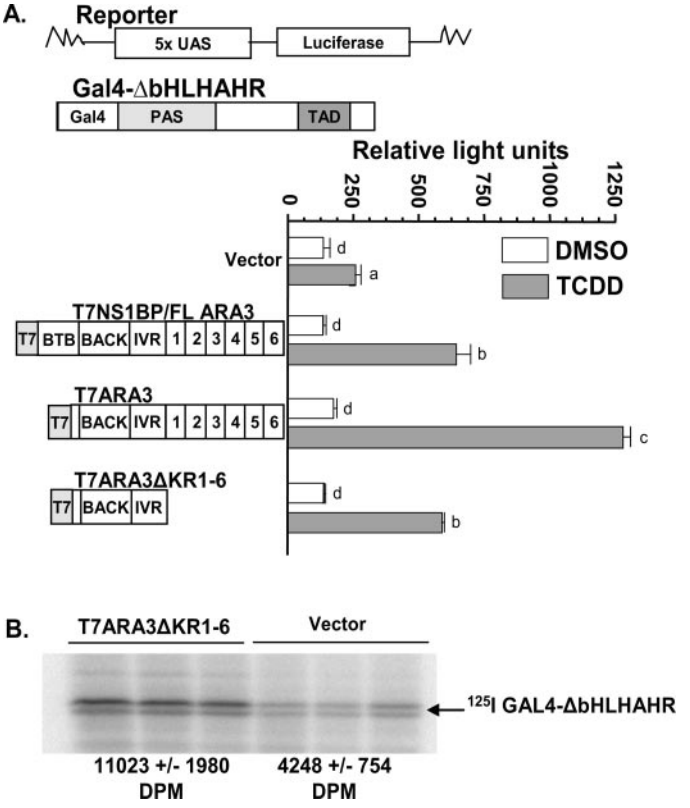

Fig. 6. ARA3 modifies signaling of an AHR chimera in mammalian cells. A, Cos-1 cells were transiently transfected with ΔbHLHAHR fused to the GAL4 DNA binding domain (Gal4-ΔbHLHAHR), a luciferase reporter, and a β-galactosidase transfection control vector. In addition, NS1BP/FLARA3, ARA3, ARA3ΔK1–6, or an empty vector was transfected into the Cos-1 cells. The cells were treated with 10 nM TCDD or vehicle, and Luciferase and LacZ activity was determined. Luciferase activity was normalized to LacZ activity. Values are the average of two replicates and represent at least two independent experiments. Statistical significance was determined with ANOVA followed by Tukey's multiple comparison test in PRISM. The same subscript depicts values that are statistically the same ($P > 0.05$). Different subscripts designate a statistical difference in the values ($P < 0.001$). B, Cos-1 cells were transiently transfected with the Gal4-AHR chimera in the presence of ARA3ΔK1–6 or an empty vector. Cytosolic protein was labeled with the photoaffinity AHR ligand and the samples were run on a 7.5% SDS-polyacrylamide gel electrophoresis gel. Gels were analyzed by autoradiography and appropriate bands were cut out and counted on a Minaxi gamma counter. Statistical significance was determined with a Student's *t* test ($P < 0.05$).

Model. Based upon the domain maps described above and what is known about other BTB-kelch proteins, a model of NS1BP in AHR signaling can be proposed. The data presented here are consistent with the idea that NS1BP/FLARA3 influences the cytosolic concentration of AHR by two mechanisms. First, NS1BP may tether AHR to the actin cytoskeleton. In this regard, it has been shown that NS1BP colocalizes with actin and can bind actin filaments through its kelch domain (Sasagawa et al., 2002). Second, the BTB domain of NS1BP may direct the proteosomal degradation of AHR. The BTB domain in some kelch proteins interacts with Cullin3, a member of the E3 ubiquitin-ligase complex (Stogios and Prive, 2004; Furukawa and Xiong, 2005). In agreement with this model is the observation that, in both yeast and mammalian cells, the NS1BP construct with a deletion of the BTB domain (i.e., ARA3) significantly increased AHR signaling compared with full-length NS1BP. That is, ARA3, without the BTB domain, may behave in a dominant-negative manner by competing with NS1BP. Likewise, the BACK/IVR domains of NS1BP alone also may function in a dominant-negative manner, albeit less effectively than ARA3 with the kelch domain that links it to the cytoplasm. In fact, we have shown that the BACK/IVR domains of NS1BP alone increase the concentration of functional AHR. In summary, NS1BP modifies AHR signaling by both positively and negatively influencing the concentration of AHR through the kelch and BTB domains, respectively.

References

Adams J, Kelso R, and Cooley L (2000) The kelch repeat superfamily of proteins: propellers of cell function. *Trends Cell Biol* **10:**17–24.

Bartel PL, Chien C, Sternglanz R, and Fields S (1993) Using the two-hybrid system to detect protein-protein interactions, in *Cellular Interactions in Development: A Practical Approach* (Hartley DA ed) pp 153–179, IRL Press, Oxford.

Beischlag TV, Wang S, Rose DW, Torchia J, Reisz-Porszasz S, Muhammad K, Nelson WE, Probst MR, Rosenfeld MG, and Hankinson O (2002) Recruitment of the NCoA/SRC-1/p160 family of transcriptional coactivators by the aryl hydrocarbon receptor/aryl hydrocarbon receptor nuclear translocator complex. *Mol Cell Biol* **22:**4319–4333.

Bell DR and Poland A (2000) Binding of aryl hydrocarbon receptor (AhR) to AhR-interacting protein. The role of hsp90. *J Biol Chem* **275:**36407–36414.

Bourne H and von Zastrow M (2001) Drug receptors and pharmacodynamics, in *Basic and Clinical Pharmacology* (Katzung B ed) pp 9–34, Lange Medical Books/McGraw-Hill, New York.

Bradfield CA, Kende AS, and Poland A (1988) Kinetic and equilibrium studies of Ah receptor-ligand binding: use of [^{125}I]2-iodo-7,8-dibromodibenzo-*p*-dioxin. *Mol Pharmacol* **34:**229–237.

Carver LA and Bradfield CA (1997) Ligand dependent interaction of the Ah receptor with a novel immunophilin homolog *in vivo*. *J Biol Chem* **272:**11452–11456.

Carver LA, Jackiw V, and Bradfield CA (1994) The 90-kDa heat shock protein is essential for Ah receptor signaling in a yeast expression system. *J Biol Chem* **269:**30109–30112.

Carver LA, LaPres JJ, Jain S, Dunham EE, and Bradfield CA (1998) Characterization of the Ah receptor-associated protein, ARA9. *J Biol Chem* **273:**33580–33587.

Collins T, Stone JR, and Williams AJ (2001) All in the family: the BTB/POZ, KRAB and SCAN domains. *Mol Cell Biol* **21:**3609–3615.

Davarinos NA and Pollenz RS (1999) Aryl hydrocarbon receptor imported into the nucleus following ligand binding is rapidly degraded via the cytosplasmic proteasome following nuclear export. *J Biol Chem* **274:**28708–28715.

Dolwick KM, Schmidt JV, Carver LA, Swanson HI, and Bradfield CA (1993) Cloning and expression of a human Ah receptor cDNA. *Mol Pharmacol* **44:**911–917.

Fernandez-Salguero PM, Hilbert DM, Rudikoff S, Ward JM, and Gonzalez FJ (1996) Aryl-hydrocarbon receptor-deficient mice are resistant to 2,3,7,8-tetrachlorodibenzo-*p*-dioxin-induced toxicity. *Toxicol Appl Pharmacol* **140:**173–179.

Furukawa M and Xiong Y (2005) BTB protein Keap1 targets antioxidant transcription factor Nrf2 for ubiquitination by the Cullin 3-Roc1 ligase. *Mol Cell Biol* **25:**162–171.

Garabedian MJ (1993) Genetic approaches to mammalian nuclear receptor function in yeast. *Methods: A Companion to Methods Enzymol* **5:**138–146.

Hogenesch JB, Chan WK, Jackiw VH, Brown RC, Gu YZ, Pray-Grant M, Perdew GH, and Bradfield CA (1997) Characterization of a subset of the basic-helix-loop-helix-PAS superfamily that interacts with components of the dioxin signaling pathway. *J Biol Chem* **272:**8581–8593.

Jain S, Dolwick KM, Schmidt JV, and Bradfield CA (1994) Potent transactivation domains of the Ah receptor and the Ah receptor nuclear translocator map to their carboxyl termini. *J Biol Chem* **269:**31518–31524.

Kazlauskas A, Poellinger L, and Pongratz I (1999) Evidence that the co-chaperone p23 regulates ligand responsiveness of the dioxin (Aryl hydrocarbon) receptor. *J Biol Chem* **274:**13519–13524.

Kozak M (1987) An analysis of 5′-noncoding sequences from 699 vertebrate messenger RNAs. *Nucleic Acids Res* **15:**8125–8132.

Kumar MB, Tarpey RW, and Perdew GH (1999) Differential recruitment of coactivator RIP140 by Ah and estrogen receptors. Absence of a role for LXXLL motifs. *J Biol Chem* **274:**22155–22164.

Lahvis GP, Pyzalski RW, Glover E, Pitot HC, McElwee MK, and Bradfield CA (2005) The aryl hydrocarbon receptor is required for developmental closure of the ductus venosus in the neonatal mouse. *Mol Pharmacol* **67:**714–720.

LaPres JJ, Glover E, Dunham EE, Bunger MK, and Bradfield CA (2000) ARA9 modifies agonist signaling through an increase in cytosolic aryl hydrocarbon receptor. *J Biol Chem* **275:**6153–6159.

Ma Q and Whitlock JP Jr (1997) A novel cytoplasmic protein that interacts with the Ah receptor, contains tetratricopeptide repeat motifs and augments the transcriptional response to 2,3,7,8-tetrachlorodibenzo-*p*-dioxin. *J Biol Chem* **272:**8878–8884.

Melnick A, Carlile G, Ahmad KF, Kiang CL, Corcoran C, Bardwell V, Prive GG, and Licht JD (2002) Critical residues within the BTB domain of PLZF and Bcl-6 modulate interaction with corepressors. *Mol Cell Biol* **22:**1804–1818.

Meyer BK, Pray-Grant MG, Vanden Heuvel JP, and Perdew GH (1998) Hepatitis B virus X-associated protein 2 is a subunit of the unliganded aryl hydrocarbon receptor core complex and exhibits transcriptional enhancer activity. *Mol Cell Biol* **18:**978–988.

Mimura J, Ema M, Sogawa K, and Fujii-Kuriyama Y (1999) Identification of a novel mechanism of regulation of Ah (dioxin) receptor function. *Genes Dev* **13:**20–25.

Petrulis JR, Hord NG, and Perdew GH (2000) Subcellular localization of the aryl hydrocarbon receptor is modulated by the immunophilin homolog hepatitis B virus X-associated protein 2. *J Biol Chem* **275:**37448–37453.

Pohjanvirta R and Tuomisto J (1994) Short-term toxicity of 2,3,7,8-tetrachlorodibenzo-*p*-dioxin in laboratory animals: effects, mechanisms and animal models. *Pharmacol Rev* **46:**483–549.

Reyes H, Reisz-Porszasz S, and Hankinson O (1992) Identification of the Ah receptor nuclear translocator protein (Arnt) as a component of the DNA binding form of the Ah receptor. *Science (Wash DC)* **256:**1193–1195.

Sasagawa K, Matsudo Y, Kang M, Fujimura L, Iitsuka Y, Okada S, Ochiai T, Tokuhisa T, and Hatano M (2002) Identification of Nd1, a novel murine kelch family protein, involved in stabilization of actin filaments. *J Biol Chem* **277:**44140–44146

Schmidt JV and Bradfield CA (1996) Ah receptor signaling pathways. *Annu Rev Cell Dev Biol* **12:**55–89.

Stogios PJ and Prive GG (2004) The BACK domain in BTB-kelch proteins. *Trends Biochem Sci* **29:**634–637.

Vojtek AB, Hollenberg SM, and Cooper JA (1993) Mammalian Ras interacts directly with the serine/threonine kinase Raf. *Cell* **74:**205–214.

Wilhelmsson A, Cuthill S, Denis M, Wikstrom AC, Gustafsson JA, and Poellinger L (1990) The specific DNA binding activity of the dioxin receptor is modulated by the 90 kd heat shock protein. *EMBO (Eur Mol Biol Organ) J* **9:**69–76.

Wolff T, O'Neill RE, and Palese P (1998) NS1-Binding protein (NS1-BP): a novel human protein that interacts with the influenza A virus nonstructural NS1 protein is relocalized in the nuclei of infected cells. *J Virol* **72:**7170–7180.

Yao G, Craven M, Drinkwater N, and Bradfield CA (2004) Interaction networks in yeast define and enumerate the signaling steps of the vertebrate aryl hydrocarbon receptor. *PLoS Biol* **2:**E65.

Zollman S, Godt D, Prive GG, Couderc JL, and Laski FA (1994) The BTB domain, found primarily in zinc finger proteins, defines an evolutionarily conserved family that includes several developmentally regulated genes in Drosophila. *Proc Natl Acad Sci USA* **91:**10717–10721.

Address correspondence to: Christopher A. Bradfield, McArdle Laboratory for Cancer Research, 1400 University Avenue, Madison, WI 53706-1599. E-mail: bradfield@oncology.wisc.edu